suggested that two brothers, aged 22 months and 7 months, from a Japanese consanguineous family reported by Sonoda and Kouno [10] would also fit the diagnosis of ATCS. The brothers had multiple distal arthrogryposis, characteristic facial features, cleft palates, short stature, hydronephrosis, cryptorchidism, and normal intelligence. Dündar et al. [9] also showed follow-up observations of the original patients: the intelligence quotient (IQ) was roughly 90 in one subject at age 7 years and 2 months and the other died of unknown cause at 5 years of age. Janecke et al. [11] from Innsbruck Medical University, Austria, reported two brothers with ATCS from a consanguineous Austrian family, one of whom died shortly after birth because of respiratory failure. The authors concluded that all these patients represented a new type of arthrogryposis with central nervous system involvement, congenital heart defects, urogenital defects, myopathy, connective tissue involvement (generalized joint laxity), and normal or subnormal mental development. In 2009, Dündar et al. reported that *CHST14* was the causal gene for ATCS through homozygosity mapping using samples from four previously published consanguineous families. The authors mentioned some follow-up clinical findings including generalized joint laxity, delayed wound healing, ecchymoses, hematomas, and osteopenia/osteoporosis; and categorized ATCS as a generalized connective tissue disorder [5].

## 2.2. EDS, Kosho type

We encountered the first patient with a specific type of EDS in 2000 and the second with parental consanguinity in 2003. They were Japanese girls with strikingly similar symptoms: characteristic craniofacial features; skeletal features including multiple congenital contractures, malfanoid habitus, pectus excavatum, generalized joint laxity, recurrent dislocations, and progressive talipes and spinal deformity; skin hyperextensibility, bruisability, and fragility with atrophic scars; recurrent hematomas; and hypotonia with mild motor developmental delay [12]. These symptoms overlapped those in the kyphoscoliosis type EDS (previously known as EDS type VI), which is typically associated with deficiency of lysyl hydroxylase (EDS type VIA) [13]. A rare condition with the clinical phenotype of the kyphoscoliosis type EDS but with normal lysyl hydroxylase activity were reported and named as EDS type VIB [13]. Therefore, we tentatively proposed that the two patients represented a clinically recognizable subgroup of EDS type VIB [12]. Through their long-term clinical evaluation as well as four additional unrelated Japanese patients including one with parental consanguinity and another reported by Yasui et al. [14], we concluded that they—four female patients and two male patients aged 4–32 years, represented a new clinically recognized type of EDS with distinct craniofacial characteristics, multiple congenital contractures, progressive joint and skin laxity, and multisystem fragility-related manifestations [15]. The disorder has been registered as EDS Kosho Type (EDSKT) in the London Dysmorphology Database (http://www.lmdatabases.com/index.html) and in POSSUM (http://www.possum.net.au/). In 2009, we identified *CHST14* as causal for the disorder through homozygosity mapping using samples from two consanguineous families and all the other patients were also found to have compound heterozygous *CHST14* mutations [6].

### 2.3. Musculocontractural EDS

Malfait et al. [7] from Ghent University, Belgium have found mutations in *CHST14* through homozygosity mapping of two Turkish sisters and an Indian girl both presenting clinically with EDS VIB and with parental consanguinity. They had distinct craniofacial features, joint contractures, and wrinkled palms in addition to common features of kyphoscoliosis type EDS including kyphoscoliosis, muscular hypotonia, hyperextensible, thin, and bruisable skin, atrophic scarring, joint hypermobility, and variable ocular involvement. Malfait et al. [7] concluded that their series and ATCS, as well as EDSKT, formed a phenotypic continuum based on their clinical observations and identification of an identical mutation in both conditions; and proposed to coin the disorder as "musculocontractural EDS" (MCEDS).

## 3. Pathophysiology of D4ST1-deficient EDS

### 3.1. Glycobiological abnormalities in D4ST1-deficient EDS

D4ST1 is a regulatory enzyme in the glycosaminoglycan (GAG) biosynthesis that transfers active sulfate to position 4 of the N-acetyl-D-galactosamine residues of dermatan sulfate (DS) (Fig. 1) [16, 17]. DS, together with chondroitin sulfate (CS) and heparan sulfate, constitutes GAG chains of proteoglycans and is implicated in cardiovascular disease, tumorigenesis, infection, wound repair, and fibrosis via DS-containing proteoglycans such as decorin and biglycan [18].

Sulfotransferase activity toward dermatan in the skin fibroblasts derived from the patients was significantly decreased to 6.7% (patient 1 with a compound heterozygous mutation: P281L/Y293C) and 14.5% (patient 3 with a homozygous mutation: P281L) of each age- and sex-matched control) (Fig. 2A). Disaccharide composition analysis of CS/DS chains isolated from the skin fibroblasts showed a negligible amount of DS and a slight excess of CS (Fig. 2B). Subsequently, we focused on a major DS proteoglycan in the skin, decorin, consisting of core protein and one GAG chain and playing an important role in assembly of collagen fibrils (Nomura, 2006). No DS disaccharides were detected in the GAG chains of decorin from the patients, whereas the GAG chains of decorin from the controls were mainly composed of DS disaccharides (approximately 95%) (Fig. 2C) [6].

### 3.2. Pathological abnormalities in D4ST1-deficient EDS

Hematoxylin and eosin (H&E)-stained light microscopy on patients' skin specimens showed that fine collagen fibers were present predominantly in the reticular to papillary dermis with marked reduction of normally thick collagen bundles (Fig. 3a, b). Electron microscopy showed that collagen fibrils were dispersed in the reticular dermis, compared with the regularly and tightly assembled ones observed in the control; whereas each collagen fibril was smooth and round, not varying in size and shape, similar to each fibril of the control (Fig. 3c, d) [6].

| Patient | Family | Origin | *CHST14* mutations | Sex | Age at initial publication | References |
|---|---|---|---|---|---|---|
| 1 | 1 | Turkish | V49X homo | F | 3.5y | [8] |
| 2 | | | | M | 1.5y | |
| 3 | | | | F | 6y | |
| 4 | 2 | Japanese | Y293C homo | M | 4y | [10] |
| 5 | | | | M | 7m | |
| 6 | 3 | Austrian | R213P homo | M | 0d† | [11] |
| 7 | | | | M | 12m | |
| 8 | 4 | Turkish | [R135G;L137Q] homo | F | 1–4m† | [9] |
| 9 | | | | M | 1–4m† | |
| 10 | | | | M | 1–4m† | |
| 11 | | | | M | 3m | |
| 12 | 5 | Japanese | P281L/Y293C | F | 11y | [12] |
| 13 | 6 | Japanese | P281L homo | F | 14y | [12] |
| 14 | 7 | Japanese | P281L homo | M | 32y | [15] |
| 15 | 8 | Japanese | K69X/P281L | M | 32y | [14,15] |
| 16 | 9 | Japanese | P281L/C289S | F | 20y | [15] |
| 17 | 10 | Japanese | P281L/Y293C | F | 4y | [15] |
| 18 | 11 | Turkish | V49X homo | F | 22y | [7] |
| 19 | | | | F | 21y | |
| 20 | 12 | Indian | E334Gfs*107 homo | F | 12y | [7] |
| 21 | 13 | Japanese | P281L/Y293C | M | 2y | [21] |
| 22 | 14 | Japanese | F209S/P281L | M | 6y | [21] |
| 23 | 15 | Dutch | V48X homo | F | 20y | [23] |
| 24 | 16 | Afghani | R274P homo | F | 11y | [24] |
| 25 | | | | F | 0y | |
| 26 | 17 | Miccosukee | G228Lfs*13 | F | 16y | [25] |

homo, homozygous mutation; /, compound heterozygous mutation; F, female; M, male; y, years old; m, months old; †, dead at the time of publication

**Table 2.** Reported patients with D4ST1-deficient EDS

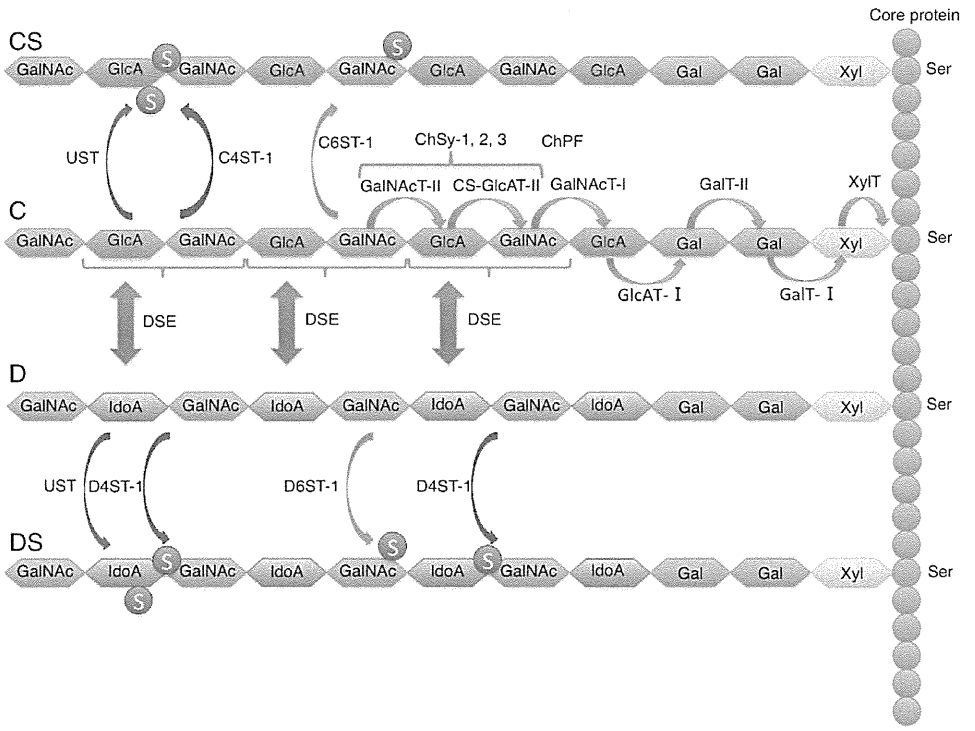


Biosynthesis of chondroitin sulfate (CS) and dermatan sulfate (DS) starts with binding a tetrasaccharide linker region, glucuronic acidβ1-3galactoseβ1-3galactoseβ1-4xyloseβ1-*O*- (GlcA-Gal-Gal-Xyl-), onto serine (Ser) residues of specific core proteins of proteoglycans, by β-xylosyltransferase (XylT), β1,4-galactosyltransferase-I (GalT-I), β1,3-galactosyltransferase-II (GalT-II), and β1,3-glucuronosyltransferase-I (GlcAT-I), respectively. Subsequently, a disaccharide chain of chondroitin (C[N-acetyl-D-galactosamine(GalNAc)-GlcA]$_n$ is synthesized by N-acetyl-D-galactosaminyltransferase-I (GalNAcT-I), N-acetyl-D-galactosaminyltransferase-II (GalNAcT-II), and CS-glucuronyltransferase-II (CS-GlcAT-II) encoded by chondroitin synthase-1, 2, 3 (ChSy-1, 2, 3); and chondroitin polymerizing factor (ChPF). CS chains are matured through sulfation by chondroitin 4-*O*-sulfotransferase-1 (C4ST-1), chondroitin 6-*O*-sulfotransferase-1 (C6ST-1), and uronyl 2-*O*- sulfotransferase (UST). A disaccharide chain of dermatan (D) is synthesized through epimerization of a carboxyl group at C5 from GlcA to L-iduronic acid (IdoA) by dermatan sulfate epimease (DSE). DS chains are matured through sulfation by dermatan 4-*O*-sulfotransferase-1 (D4ST-1), dermatan 6-*O*-sulfotransferase-1 (D6ST-1), and UST. D4ST-1 deficiency, resulting in impaired 4-*O*-sulfation lock, probably allows back epimerization from IdoA to GlcA and finally leads to loss of DS and excess of CS.

**Figure 1.** Biosynthesis of dermatan sulfate and chondroitin sulfate.

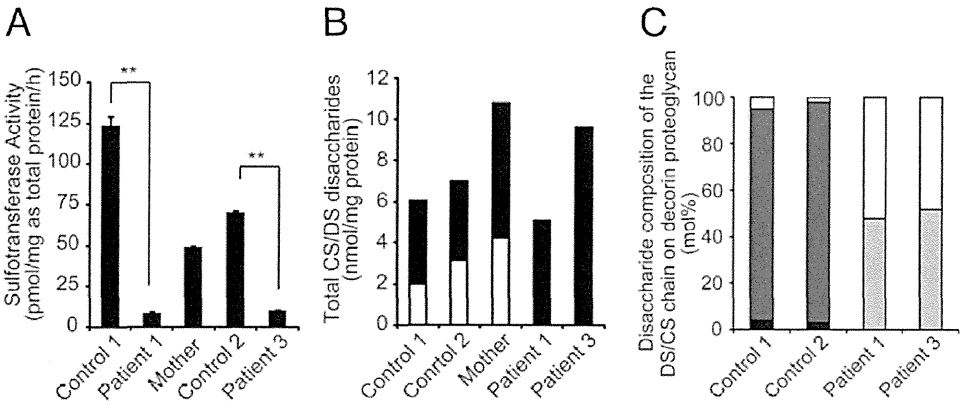


A. Sulfotransferase activity of skin fibroblasts: A patient (a compound heterozygous mutation, P281L/Y293C; patient 1), her heterozygous mother, and her age-matched control (control 1); another patient (a homozygous mutation, P281L; patient 3) and his age-matched control (control 2). B. The total amounts of CS and DS derived from skin fibroblasts. The total disaccharide contents of CS and DS are shown in a black box and a white box, respectively. C. Proportion of the disaccharide units in the CS/DS hybrid chains in decorin secreted by the fibroblasts. A white box and a light gray box indicate GlcUA-GalNAc (4S) and GlcUA-GalNAc (6S), respectively, both composing CS. A dark gray box and a black box indicate IdoUA-GalNAc(4S) and IdoUA-GalNAc (6S), respectively, both composing DS.

**Figure 2.** Glycobiological studies [6].

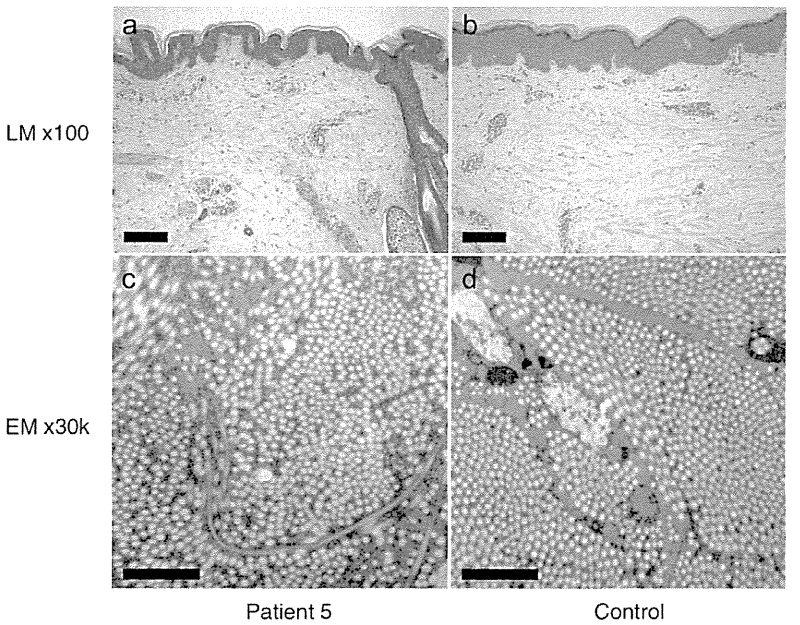


H&E-stained light microscopy (LM) on skin specimens of a patient (a compound heterozygous mutation, P281L/C289S; patient 5) (a) and an age- and sex-matched control (b). Scale bars indicate 500 μm. Electron microscopy (EM) of the patient (c) and the control (d). Scale bars indicate 1 μm.

**Figure 3.** Pathological studies [6].

In view of these glycobiological and pathological findings, skin fragility in this disorder is suggested to be caused by impaired assembly of collagen fibrils resulting from loss of DS in the GAG chain of decorin [6]. Decorin DS regulates the interfibrillar distance in collagen fibrils and permits the extracellular matrix to resist physical stress, possibly through electrostatic interaction between decorin DS chains and adjacent collagen fibrils (Fig. 4A) [19]. Collagen fibrils are dispersed in patients' skin tissues where the decorin GAG chains are exclusively composed of CS (Fig. 4B), whereas collagen fibrils in controls' skin specimens are tightly assembled through the GAG chains of decorin exclusively composed of DS (Fig. 4A).

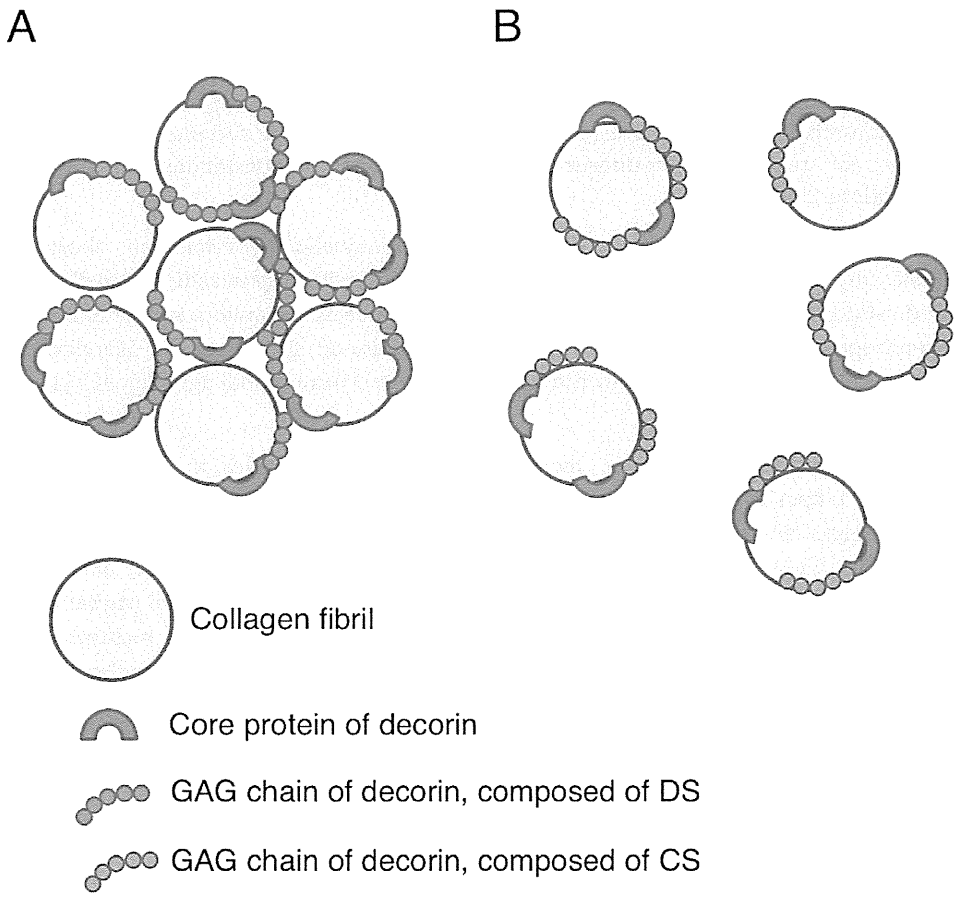


Possible relationship between collagen fibrils and decorin in skin specimens of normal control subjects (A) and of patients (B).

**Figure 4.** Schema of binding model of decorin to collagen fibrils [20].

## 4. Delineation of D4ST1-deficient EDS

Independently identified three conditions, ATCS, EDSKT, and MCEDS caused by loss-of-function mutations in CHST14, were supposed to be a single clinically recognizable type of connective tissue disorder [7, 21]. Shimizu et al. [22] presented detailed clinical information of two additional unrelated patients and a comprehensive review of all reported 20 patients, which could definitely unite the three conditions named as "D4ST1-deficient EDS (DD-EDS)". Kosho et al. [23] concluded that categorization of the disorder into a form of "EDS" was appropriate clinically because the disorder satisfied all the hallmarks of EDS including skin hyperextensibility, joint hypermobility, and tissue fragility affecting the skin, ligaments, joints, blood vessels, and internal organs [1] and etiologically because multisystem fragility in the disorder was illustrated to be caused by impaired assembly of collagen fibrils resulting from loss of DS in the decorin GAG chains [6].

To date, 26 patients have been reported to have homozygous or compound heterozygous CHST14 mutations (Table 2) [24, 25, 26]. Clinical characteristics are summarized in Table 3, consisting of progressive multisystem fragility-related manifestations and various malformations [23].

Characteristic craniofacial features including large fontanelle, hypertelorism, short and downslanting palpebral fissures, blue sclerae, short nose with hypoplastic columella, low-set and rotated ears, high palate, long philtrum, thin upper lip vermilion, small mouth, and micro-retrognathia are noted at birth to early childhood (Fig. 5A, B). Slender and asymmetrical facial shapes with protruding jaws are noted from school age (Fig. 5C) [12. 15, 22].

Congenital multiple contractures, most specifically adduction-flexion contractures of thumbs and talipes equinovarus, were cardinal features (Fig. 5D, G, J, K, M). In childhood, peculiar fingers described as "tapering", "slender", and "cylindrical" are also common features (Fig. 5E, F, H, I). Talipes deformities (planus, valgus) (Fig. 5L, N) and spinal deformities (scoliosis, kyphoscoliosis) with tall vertebral bodies and decreased physiological curvature (Fig. 5O, P, Q, R, S, T) occur and progress. Malfanoid habitus, recurrent joint dislocations, and pectus deformities (flat and thin, excavatum, carinatum) are also evident [12. 15, 22].

Cutaneous features include hyperextensibility (Fig. 5U, V) to redundancy (Fig. 5W), bruisability, fragility leading to atrophic scars, acrogeria-like fine palmar creases or wrinkles (Fig. 5F, I), hyperalgesia to pressure, and recurrent subcutaneous infections with fistula formation (Kosho et al., 2005; Kosho et al., 2010; Shimizu et al., 2011).

Recurrent large subcutaneous hematomas are the most serious complication , which sometimes progress acutely and massively to be treated intensively (admission, blood transfusion, surgical drainage) and are supposed to be caused by rupture of subcutaneous arteries or veins (Fig. 5X) [12. 15, 22].

| | |
|---|---|
| ***Craniofacial*** | ***Cardiovascular*** |
| Large fontanelle (early choldhood) | Congenital heart defects (ASD) |
| Hypertelorism | Valve abnormalities (MVP, MR, AR, ARD) |
| Short and downslanting palpebral fissures | Large subcutaneous hematomas |
| Blue sclerae | ***Gastrointestinal*** |
| Short nose with hypoplastic columella | Constipation |
| Ear deformities (prominent, posteriorly rotated, low-set) | Diverticula perforation |
| Palatal abnormalities (high, cleft) | ***Respiratory*** |
| Long philtrum and thin upper lip | (Hemo)pneumothorax |
| Small mouth/micro-retrognathia (infancy) | ***Urogenital*** |
| Slender face with protruding jaw (from school age) | Nephrolithiasis/cystolithiasis |
| Asymmetric face (from school age) | Hydronephrosis |
| ***Skeletal*** | Dilated/atonic bladder |
| Marfanoid habitus/slender build | Inguinal hernia |
| Congenital multiple contractures (fingers, wrists, hips, feet) | Cryptorchidism |
| Recurrent/chronic joint dislocations | Poor breast development |
| Pectus deformities (flat, excavated) | ***Ocular*** |
| Spinal deformities (scoliosis, kyphoscoliosis) | Strabismus |
| Peculiar fingers (tapering, slender, cylindrical) | Refractive errors (myopia, astigmatism) |
| Progressive talipes deformilies (valgus, planus, cavum) | Glaucoma/elevated intraocular pressure |
| ***Cutaneous*** | Microcornea/microphthalmia |
| Hyperextensibility/redundancy | Retinal detachment |
| Bruisability | ***Hearing*** |
| Fragility/atrophic scars | Hearing impairment |
| Fine/acrogeria-like palmar creases | ***Neurological*** |
| Hyperalgesia to pressure | Ventricular enlargement/asymmetry |
| Recurrent subcutaneous infections/fistula | ***Development*** |
| | Hypotonia/gross motor delay. |

ASD, atrial septal defect; MVP, mitral valve prolapse; MR, mitral valve regurgitation; AR, aortic valve regurgitation; ARD, aortic rot dilation

**Table 3.** Clinical manifestations in DD-EDS [23]

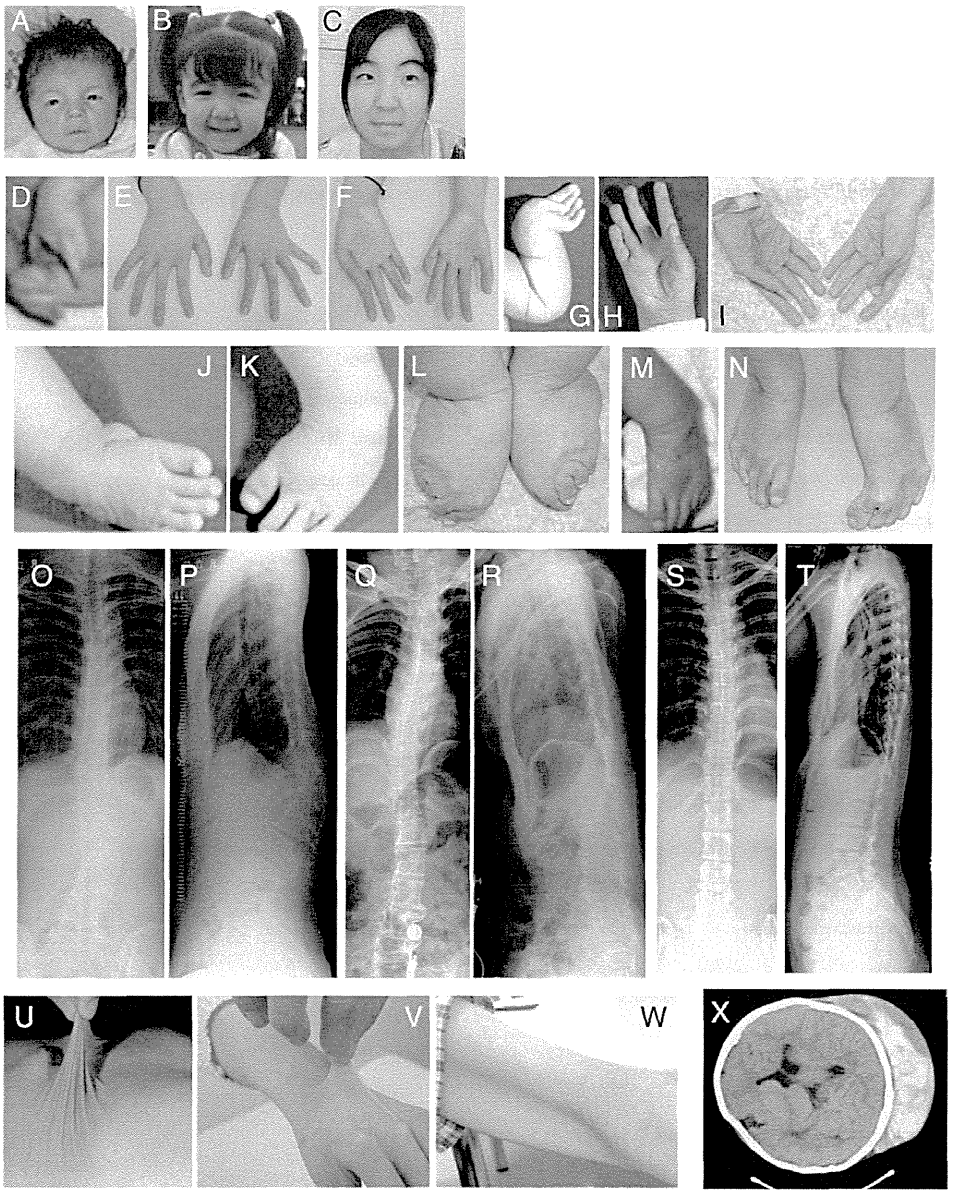


**Figure 5.** Clinical photographs of patients with DD-EDS [12, 15]. Patient 12 at birth (D), at age 23 days (A), 3 years (B), 6 years (X), and 16 years (C, E, F, O, P). Patient 13 at age 2 months (J, K), 3 months (G), 14 months (U), 5 years (H), and 28 years (I, L, Q, R). Patient 14 in the neonatal period (M) and at age 28 years (N, W). Patient 16 at age 19 years (S, T, V). Patient number is according to Table 2.

## 5. Conclusion

DD-EDS is a newly recognized and delineated form of EDS, characterized by progressive multisystem fragility-related manifestations (skin hyperextensibilty and fragility, progressive spinal and foot deformities, large subcutaneous hematoma) and various malformations (facial features, congenital eye/heart/gastrointestinal defects, congenital multiple contractures). The cause of multisystem connective tissue fragility is supposed to be impaired assembly of collagen fibrils resulting from loss of DS in the decorin GAG chains. It is the first human disorder affecting biosynthesis of DS, which emphasize a role for DS in human development and extracellular matrix maintenance [27].

## Author details

Tomoki Kosho
*Department of Medical Genetics, Shinshu University School of Medicine, Asahi, Matsumoto, Japan*

## Acknowledgement

The author is thankful to all the patients and their families for participating in this study. The authors also express the gratitude to all the collaborators. All the studies were supported by Research on Intractable Diseases from Japanese Ministry of Health, Welfare, and Labor.

## 6. References

[1] Steinmann B, Royce PM, Superti-Furga A. 2002. The Ehlers–Danlos syndrome. In: Royce PM, Steinmann B, editors. Connective tissue and its heritable disorders. New York: Wiley-Liss, p431–523.

[2] Mao JR, Bristow J. 2001. The Ehlers-Danlos syndrome: on beyond collagens. J Clin Invest 107:1063-1069.

[3] Beighton P, De Paepe A, Steinmann B, Tsipouras P, Wenstrup R. 1998. Ehlers–Danlos syndromes: revised nosology, Villefranche, 1997. Am J Med Genet 77:31–37.

[4] De Paepe A, Malfait F. 2012. The Ehlers-Danlos syndrome, a disorder with many faces. Clin Genet 82:1-11.

[5] Dündar M, Müller T, Zhang Q, Pan J, Steinmann B, Vodopiutz J, Gruber R, Sonoda T, Krabichler B, Utermann G, Baenziger JU, Zhang L, Janecke AR. 2009. Loss of dermatan-4-sulfotransferase 1 function results in adducted thumb-clubfoot syndrome. Am J Hum Genet 85:873–882.

[6] Miyake N, Kosho T, Mizumoto S, Furuichi T, Hatamochi A, Nagashima Y, Arai E, Takahashi K, Kawamura R, Wakui K, Takahashi J, Kato H, Yasui H, Ishida T, Ohashi H, Nishimura G, Shiina M, Saitsu H, Tsurusaki Y, Doi H, Fukushima Y, Ikegawa S, Yamada S, Sugahara K. Matsumoto N. 2010. Loss-of-function mutations of *CHST14* in a new type of Ehles–Danlos syndrome. Hum Mutat 31:966–974.

[7] Malfait F, Syx D, Vlummens P, Symoens S, Nampoothiri S, Hermanns-Lê, Van Lear L, De Paepe A. Musculocontractural Ehlers–Danlos syndrome (former EDS type VIB) and adducted thumb clubfoot syndrome (ATCS) represent a single clinical entity caused by mutations in the dermatan-4-sulfotransferase 1 encoding *CHST14* gene. 2010. Hum Mutat 31:1233–1239.

[8] Dündar M, Demiryilmaz F, Demiryilmaz I, Kumandas S, Erkilic K, Kendirch M, Tuncel M, Ozyazgan I, Tolmie JL. 1997. An autosomal recessive adducted thumb-club foot syndrome observed in Turkish cousins. Clin Genet 51:61–64.

[9] Dündar M, Kurtoglu S, Elmas B, Demiryilmaz F, Candemir Z, Ozkul Y, Durak AC. 2001. A case with adducted thumb and club foot syndrome. Clin Dysmorphol 10:291–293.

[10] Sonoda T, Kouno K. 2000. Two brothers with distal arthrogryposis, peculiar facial appearance, cleft palate, short stature, hydronephrosis, retentio testis, and normal intelligence: a new type of distal arthrogryposis? Am J Med Genet 91:280–285.

[11] Janecke AR, Unsinn K, Kreczy A, Baldissera I, Gassner I, Neu N, Utermann G, Müller T. 2001. Adducted thumb-club foot syndrome in sibs of a consanguineous Austrian family. J Med Genet 38:265–269.

[12] Kosho T, Takahashi J, Ohashi H, Nishimura G, Kato H, Fukushima Y. 2005. Ehlers–Danlos syndrome type VIB with characteristic facies, decreased curvatures of the spinal column, and joint contractures in two unrelated girls. Am J Med Genet Part A 138A:282–287.

[13] Yeowell HN, Steinmann B. 2008. Ehlers-Danlos Syndrome, Kyphoscoliotic Form. n: Pagon RA, Bird TD, Dolan CR, Stephens K, Adam MP, editors. GeneReviews™ [Internet]. Seattle (WA): University of Washington, Seattle; 1993-.2000 Feb 02 [updated 2008 Feb 19].

[14] Yasui H, Adachi Y, Minami T, Ishida T, Kato Y, Imai K. 2003. Combination therapy of DDAVP and conjugated estrogens for a recurrent large subcutaneous hematoma in Ehlers–Danlos syndrome. Am J Hematol 72:71–72.

[15] Kosho T, Miyake N, Hatamochi A, Takahashi J, Kato H, Miyahara T, Igawa Y, Yasui H, Ishida T, Ono K, Kosuda T, Inoue A, Kohyama M, Hattori T, Ohashi H, Nishimura G, Kawamura R, Wakui K, Fukushima Y, Matsumoto N. 2010. A new Ehlers–Danlos syndrome with craniofacial characteristics, multiple congenital contractures, progressive joint and skin laxity, and multisystem fragility-related manifestations. Am J Med Genet Part A 152A:1333–1346.

[16] Evers MR, Xia G, Kang HG, Schachner M, Baeziger JU. 2001. Molecular cloning and characterization of a dermatan-specific *N*-acetylgalactosamine 4-O-sulfotransferase. J Biol Chem 276:36344–36353.

[17] Mikami T, Mizumoto S, Kago N, Kitagawa H, Sugahara K. 2003. Specificities of three distinct human chondroitin/dermatan *N*-acetylgalactosamine 4-O-sulfotransferases demonstrated using partially desulfated dermatan sulfate as an acceptor: implication of differential roles in dermatan sulfate biosynthesis. J Biol Chem 278:36115–36127.

[18] Trowbridge JM, Gallo RL. 2002. Dermatan sulfate: new functions from an old glycosaminoglycan. Glycobiol 12:117R–25R.

[19] Nomura Y. 2006. Structural changes in decorin with skin aging. Connect Tissue Res 47:249–255.

[20] Kosho T. 2011. Discovery and delineation of a new type of Ehlers-Danlos syndrome caused by dermatan 4-*O*-sulfotransferase deficiency. Shinshu Med J 59:305-319.

[21] Janecke AR, Baenziger JU, Müller T, Dündar M. 2011. Letter to the Editors. Loss of dermatan-4-sulfotransferase 1 (D4ST1/*CHST14*) function represents the first dermatan sulfate biosynthesis defect, "Dermatan sulfate-deficient adducted thumb-clubfoot syndrome". Hum Mutat 32:484–485.

[22] Shimizu K, Okamoto N, Miyake N, Taira K, Sato Y, Matsuda K, Akimaru N, Ohashi H, Wakui K, Fukushima Y, Matsumoto N, Kosho T. 2011. Delineation of dermatan 4-O-sulfotransferase 1 deficient Ehlers-Danlos syndrome: observation of two additional patients and comprehensive review of 20 reported patients. Am J Med Genet Part A 155:1949-1958

[23] Kosho T, Miyake N, Mizumoto S, et al. 2011. A response to: loss of dermatan-4-sulfotransferase 1 (D4ST1/CHST14) function represents the first dermatan sulfate biosynthesis defect, "dermatan sulfate-deficient Adducted Thumb-Clubfoot Syndrome". Which name is appropriate, "Adducted Thumb-Clubfoot Syndrome" or "Ehlers-Danlos syndrome"? Hum Mutat 32:1507-1509.

[24] Voermans NC, Kempers M, Lammens M, van Alfen N, Janssen MC, Bönnemann C, van Engelen BG, Hamel BC. 2012. Myopathy in a 20-year-old female patient with D4ST-1 deficient Ehlers-Danlos syndrome due to a homozygous CHST14 mutation. Am J Med Genet A 158A:850-855.

[25] Mendoza-Londono R, Chitayat D, Kahr WH, Hinek A, Blaser S, Dupuis L, Goh E, Badilla-Porras R, Howard A, Mittaz L, Superti-Furga A, Unger S, Nishimura G, Bonafe L. 2012. Extracellular matrix and platelet function in patients with musculocontractural Ehlers-Danlos syndrome caused by mutations in the *CHST14* gene. Am J Med Genet A 158A:1344-1354.

[26] Winters KA, Jiang Z, Xu W, Li S, Ammous Z, Jayakar P, Wierenga KJ. 2012. Re-assigned diagnosis of D4ST1-deficient Ehlers-Danlos syndrome (adducted thumb-clubfoot syndrome) after initial diagnosis of Marden-Walker syndrome. Am J Med Genet A 158A:2935-2940.

[27] Zhang L, Müller T, Baenziger JU, Janecke AR. 2010. Congenital disorders of glycosylation with emphasis on loss of dermatan-4-sulfotransferase? 93:289–307.

*Human Molecular Genetics, 2013, Vol. 22, No. 18* **3761–3772**
*doi:10.1093/hmg/ddt227*
*Advance Access published on May 23, 2013*

# Loss of dermatan sulfate epimerase (DSE) function results in musculocontractural Ehlers–Danlos syndrome

**Thomas Müller[1,†], Shuji Mizumoto[4,†], Indrajit Suresh[5,†], Yoshie Komatsu[4], Julia Vodopiutz[6], Munis Dundar[7], Volker Straub[8], Arno Lingenhel[2], Andreas Melmer[3], Silvia Lechner[2], Johannes Zschocke[2], Kazuyuki Sugahara[4] and Andreas R. Janecke[1,2,*]**

[1]Department of Pediatrics I, [2]Division of Human Genetics and [3]Department of Internal Medicine I, Innsbruck Medical University, Innsbruck, Austria, [4]Laboratory of Proteoglycan Signaling and Therapeutics, Frontier Research Center for Post- Genomic Science and Technology, Graduate School of Life Science, Hokkaido University, Sapporo, Japan, [5]Jagadguru Sri Shivarathreeshwara University Hospital, Mysore, Karnataka, India, [6]Department of Pediatrics and Adolescent Medicine, Medical University of Vienna, Vienna, Austria, [7]Department of Medical Genetics, Erciyes University, Talas, Kayseri, Turkey and [8]Institute of Genetic Medicine, Newcastle University, Central Parkway, Newcastle upon Tyne NE1 3BZ, UK

Received March 17, 2013; Revised and Accepted May 16, 2013

**The sulfated polysaccharide dermatan sulfate (DS) forms proteoglycans with a number of distinct core proteins. Iduronic acid-containing domains in DS have a key role in mediating the functions of DS proteoglycans. Two tissue-specific DS epimerases, encoded by *DSE* and *DSEL*, and a GalNAc-4-*O*-sulfotransferase encoded by *CHST14* are necessary for the formation of these domains. *CHST14* mutations were previously identified for patients with the musculocontractural type of Ehlers–Danlos syndrome (MCEDS). We now identified a homozygous *DSE* missense mutation (c.803C>T, p.S268L) by the positional candidate approach in a male child with MCEDS, who was born to consanguineous parents. Heterologous expression of mutant full-length and soluble recombinant DSE proteins showed a loss of activity towards partially desulfated DS. Patient-derived fibroblasts also showed a significant reduction in epimerase activity. The amount of DS disaccharides was markedly decreased in the conditioned medium and the cell fraction from cultured fibroblasts of the patient when compared with a healthy control subject, whereas no apparent difference was observed in the chondroitin sulfate (CS) chains from the conditioned media. However, the total amount of CS disaccharides in the cell fraction from the patient was increased ~1.5-fold, indicating an increased synthesis or a reduced conversion of CS chains in the cell fraction. Stable transfection of patient fibroblasts with a *DSE* expression vector increased the amount of secreted DS disaccharides. DSE deficiency represents a specific defect of DS biosynthesis. We demonstrate locus heterogeneity in MCEDS and provide evidence for the importance of DS in human development and extracellular matrix maintenance.**

## INTRODUCTION

Proteoglycans are formed by covalent attachments of glycosaminoglycans (GAGs), long chains composed of repeating disaccharide subunits such as dermatan sulfate (DS), chondroitin sulfate (CS) and heparan sulfate (HS), to serine residues of core proteins. Proteoglycans are major components of the extracellular matrix and contribute to normal embryonic and postnatal development and tissue homoeostasis by ensuring tissue stability and signaling functions. For example, the negative

*To whom correspondence should be addressed at: Department of Pediatrics I, Division of Human Genetics, Innsbruck Medical University, Anichstrasse 35, A-6020 Innsbruck, Austria. Tel: +43 51250482415; Fax: +43 51250424934; Email: andreas.janecke@i-med.ac.at
†The authors wish it to be known that, in their opinion, the first three authors should be regarded as joint First Authors.

charge of GAGs provides hydrophilic properties, and the accumulating water mechanically ensures an appropriate elastic tissue tonus; the small DS proteoglycans biglycan and decorin are known for their roles in forming and modifying collagen fibers in size and organization. Mature proteoglycans and unbound GAGs have also been implicated in modulating growth factor signaling (1–6). DS GAGs and DS proteoglycans interact with and modulate the activity of signaling molecules participating in cell adhesion, migration, proliferation, neurite outgrowth, wound repair and anticoagulant processes (5,7–10). A widespread distribution of DS proteoglycans in mammalian tissues has been described including blood vessel walls, skin, tendon, sclera, cartilage and undifferentiated mesenchymal tissues (11). Recent studies have also revealed roles of CS/DS chains in the orchestration of the neural stem/progenitor cell micromilieu (12).

A basic outline of CS/DS biosynthesis is summarized in Figure 1. A covalent tetrasaccharide linkage sequence (glucuronic acid–galactose–galactose–xylose-*O*–) is common to the formation of HS, CS and DS proteoglycans and results from the actions of four distinct monosaccharide transferases (13). The type of GAGs synthesized is then defined by the composition of the GAG chains added to the linker tetrasaccharide of the corresponding proteoglycans (Fig. 1).

CS is synthesized by the action of CS synthases, which alternately add *N*-acetyl-D-galactosamine (GalNAc) and D-glucuronic acid (GlcUA) residues to the tetrasaccharide linkage region. DS and CS/DS hybrid GAG chains are produced by the epimerization of the CS C-5 hydroxy of a number of GlcUA residues to L-iduronic acid (IdoUA) by glucuronyl C5-epimerases (14). Two genes encoding chondroitin-glucuronate C5-epimerases (EC 5.1.3.19), DSE (dermatan sulfate epimerase, DS-epi1, SART2, squamous cell carcinoma antigen recognized by T cell 2, [MIM 605942]) and DSEL (dermatan sulfate epimerase like, DS-epi2, [MIM 611125]), respectively, are present in organisms ranging from *Xenopus tropicalis* to humans but not in worms or flies (15). These enzymes can catalyze the epimerization of the C-5 hydroxy in both directions; the addition of sulfate to the C-4 hydroxy of the adjacent GalNAc to IdoUA or GlcUA hinders further epimerization of these residues (16). Four GalNAc-4-*O*-sulfotransferases have been cloned that act on CS and/or DS, chondroitin 4-*O*-sulfotransferases 1–3 (CHST11 [MIM 610128], CHST12 [MIM 610129], CHST13 [MIM 610124]) (17–19) and dermatan-4-*O*-sulfotransferase 1 (CHST14 [MIM 608429]) (20,21). DS and CS can be further modified by the addition of sulfate to the C-2 hydroxy of IdoUA and GlcUA, and to C-6 hydroxy of GalNAc (22). Both the degree of DS sulfation and the proportions of IdoUA and GlcUA vary spatiotemporarily, and increase the structural and functional diversity of proteoglycans (10,23).

The Ehlers–Danlos syndromes (EDSs) represent a clinically and genetically heterogeneous group of diseases, which are characterized by fragility of the soft connective tissues. The clinical spectrum varies from mild skin and joint hyperlaxity to severe physical disability, and to life-threatening vascular complications. Mutations in genes encoding fibrillar collagens or enzymes

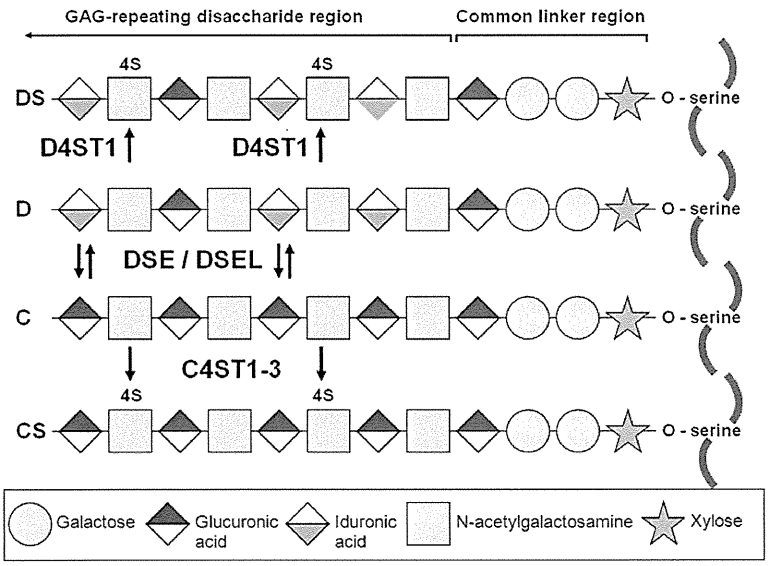


**Figure 1.** Biosynthesis of DS and chondroitin sulfate (CS). CS, DS and also HS share the synthesis of a tetrasaccharide linker region that attaches the glycosaminoglycan chains to a serine residue within the conserved attachment site of core proteins. The activity of a unique *N*-acetylgalactosaminyltransferase-I (GalNAcT-I) that transfers the first GalNAc residue onto the tetrasaccharide linker starts a growing glycosaminoglycan chain to CS. This step is followed by the activities of specific enzymes that polymerize the glycosaminoglycan chain by the alternate additions of *N*-acetyl-D-galactosamine (GalNAc) and D-glucuronic acid (GlcUA) moieties in CS. CS chains can be modified during elongation by Golgi residents, epimerase and a number of sulfotransferases. After the formation of the chondroitin backbone, epimerization of GlcUA to L-iduronic acid (IdoUA) by C5-hydroxyl epimerases (DSE or DSEL) followed by sulfate addition to the C4 hydroxy of the adjacent GalNAc residue by D4ST1 generates DS from CS, and prevents back-epimerization of IdoUA to GlcUA. In CS sequences, the C4 hydroxy of the GalNAc residue adjacent to GlcUA can be sulfated by specific CS/DS sulfotransferases C4ST1, -2 and -3. The extent of modification with sulfate groups by the actions of CS/DS sulfotransferases varies between different core proteins, and spatio-temporally. All sulfotransferases transfer a sulfate group from 3′-phosphoadenosine 5′-phosphosulfate (PAPS), a universal sulfate donor to the respective sugar residue.

involved in post-translational modification of collagens account for most forms of EDSs. Six EDS subtypes are currently distinguished based on combinations of clinical symptoms, inheritance pattern and the nature of the underlying biochemical and molecular defect(s) (Villefranche classification) (24). However, the recent identification of new EDS genes would justify a revision of the Villefranche classification (25).

We recently described loss-of-function mutations in *CHST14*, resulting in dermatan 4-*O*-sulfotransferase 1 (D4ST1) deficiency, as the first disorder resulting from impaired DS biosynthesis (26,27). D4ST1 deficiency causes a clinically recognizable form of EDS, referred to as D4ST1-deficient EDS or musculocontractural EDS (MCEDS; [MIM 601776]) (28). However, a number of different terms have been used in the past for this condition. Adducted thumb-clubfoot syndrome (ATCS) (26,29–31), Kosho Type of EDS (27,32,33), Dündar syndrome, as well as kyphoscoliosis EDS without lysyl hydroxylase deficiency (EDS VIB) and distal arthrogryposis with peculiar facies and hydronephrosis are terms that have been used to describe this disorder. The recent reporting of patients with *CHST14* mutations and in-depth reviews of clinical findings support the notion that the disorders listed above all constitute a single, clinically recognizable form of EDS (28,34–37). The disorder is characterized by progressive multisystem fragility-related manifestations resulting from impaired assembly of collagen fibrils—i.e. joint dislocations and deformities, skin hyperextensibility, bruisability and fragility—and recurrent large subcutaneous hematomas, and frequently by cardiac valvular, respiratory, gastrointestinal and ophthalmological complications. Various malformations, i.e. distinct craniofacial features, multiple congenital contractures, and congenital defects in cardiovascular, gastrointestinal, renal, ocular and central nervous systems, might either result from impaired assembly of collagen fibrils or might result from deranged signaling pathways during development. In addition, a myopathy featuring muscle hypoplasia, muscle weakness and an abnormal muscle fiber pattern on histology in adulthood has been recognized in MCEDS (38), similarly as in other EDS types (39–41), and probably contributes to the gross motor developmental delay in this type of EDS.

In this study, we identified a homozygous *DSE* mutation p.S268L in a patient with MCEDS. We demonstrate that the mutation affects the epimerase's activity in that (i) patient-derived fibroblasts show a significant reduction in epimerase activity towards partially desulfated DS; (ii) heterologous expression of mutant full-length and soluble recombinant DSE proteins in COS-7 cells show an activity decreased to mock control levels towards partially desulfated DS despite wild-type expression levels; (iii) we revealed decreased cellular and secreted DS levels, similar to changes seen in D4ST1 deficiency, and an increase in cellular CS levels in the patient's fibroblasts; and (iv) stable transfection-related expression of wild-type DSE increased the amount of DS disaccharide secreted by patient fibroblasts. Our work reveals locus heterogeneity in MCEDS, and shows that DSE and D4ST1 act in concert to form IdoUA stretches in chondroitin, thereby producing mixed CS/DS and DS GAG chains, in a large number of human connective tissues. DSE deficiency is likely to affect many types of proteoglycans, which might explain the complex phenotype.

## RESULTS

### Identification of a *DSE* missense mutation in a MCEDS patient without *CHST14* mutation

A diagnosis of MCEDS was made in a cognitively normal boy at 2 years of age based on the presence of characteristic facial features, congenital contractures of the thumbs and the feet, hypermobility of finger, elbow, and knee joints and a tendency to atrophic scarring of the skin (Fig. 2). The finding of muscle weakness suggested a myopathy in the patient.

Sequence analysis of *CHST14*, the gene found to be mutated in all 23 MCEDS patients reported to-date, revealed no mutations. Considering locus heterogeneity in MCEDS, we next determined the localization of homozygous genomic regions in this offspring of consanguineous parents by high-density SNP array genotyping. We found that 19.54% of the patient's genome was homozygous, with 25 homozygous regions exceeding 4 Mb in size (data not shown). *CHST14* did not localize within a homozygous region, further excluding this gene as causing the disease in our patient. We next selected *DSE*, localizing to the largest homozygous region (44.689 Mb in size), on the basis of its known function in DS biosynthesis as a candidate for mutation analysis. We identified a homozygous *DSE* missense mutation, c.803C>T (p.S268L, Supplementary Material, Fig. S1), in the patient. Both parents and a healthy brother were

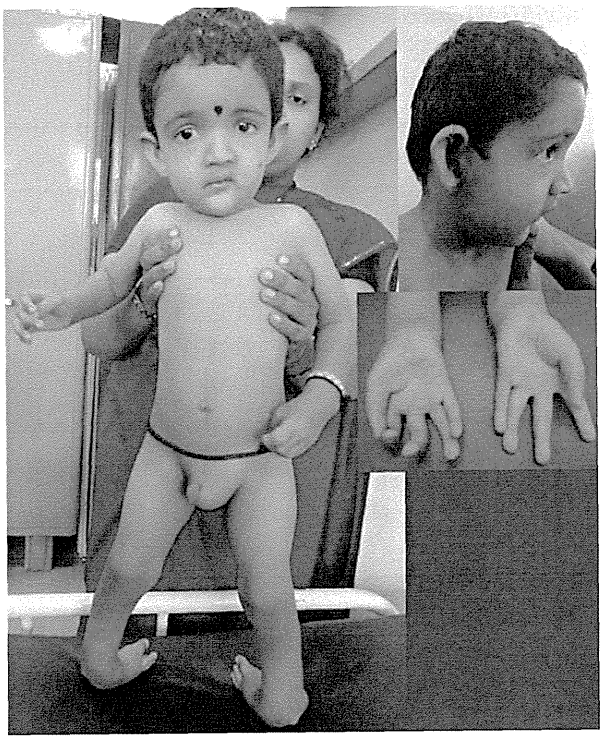

**Figure 2.** Clinical features of MCEDS due to DSE deficiency. Indian patient homozygous for DSE mutation p.S268L at age 2 years. Note characteristic facial features (see text), brachycephaly, long and tapering fingers, excessively wrinkled palms and clubfeet.

heterozygous for this mutation. This mutation is predicted by PolyPhen-2 to probably damage the protein function (HumVar score of 0.994), and was absent from the 1000 genomes, dbSNP and the NHLBI Exome Sequencing Project databases (queried on 2013-03-07), as well as from 300 Caucasian in-house control samples. Serine-268 in DSE was found to represent a highly conserved residue in DSE orthologs and in human DSEL (Supplementary Material, Fig. S2).

*DSE* had been originally cloned as a gene encoding a squamous cell carcinoma antigen recognized by cells of the HLA-A24-restricted and tumor-specific cytotoxic T-lymphocyte line; the gene was named SART2 (squamous cell carcinoma antigen recognized by T cells 2) but not assigned any specific function at the time (42). In 2006, the SART2 protein was independently purified from bovine spleen microsomes, identified by mass spectrometry, and shown to convey DS epimerase activity (15). *DSE* encodes a protein of 958 amino acids, which shares a conserved ~700 amino acid domain with DSEL; significant homology is further observed with bacterial alginate oligo-lyases (UniProtKB accession numbers 3A0O, 3AFL). Lyase and epimerase reactions are mechanistically related and are at times expressed by a single protein (e.g. alginate AlgE7) (43). No sequence similarity is observed with HS epimerases (14). Consistent with the role of a GAG-modifying enzyme, and the predictions of an N-terminal endoplasmic reticulum (ER) membrane retention signal and an N-terminal transmembrane domain, subcellular localization analyses of tagged DSE and immunoprecipitation experiments indicated localization in ERs and in part in Golgi. DS epimerase activity is ubiquitously present in normal tissues, although with quantitative differences (15). In mice, DSE contributes to the major part of enzyme activity in extracts of most tissues, with the lowest expression in the brain (44).

### The identified *DSE* mutation causes loss of epimerase activity

We hypothesized that the DSE mutation p.S268L compromised epimerase function and caused MCEDS in our patient. This was investigated by assaying epimerase activity towards partially desulfated DS as an acceptor in patient and control fibroblasts, and in COS-7 cells transiently over-expressing full-length and soluble recombinant mutant and wild-type enzymes, respectively.

Our strategy for the characterization of DSE reaction products is shown in Supplementary Material, Figure S3, and the substrate specificity of bacterial chondroitinases used in this study is shown in Supplementary Material, Figure S4. DSE catalyzes the epimerization of GlcUA into IdoUA in chondroitin chains and the reverse reaction in dermatan chains. Microsomal DSE preparations from fibroblasts showed a higher epimerase activity toward the carboxy group of IdoUA than GlcUA *in vitro* (45), i.e. the reverse reaction is favored. Thus, extrinsic dermatan rather than chondroitin was utilized as substrate for the DSE assay.

Heterologous expression of mutant full-length recombinant DSE proteins showed an activity decreased to mock control levels towards partially desulfated DS despite wild-type expression levels (Fig. 3). A soluble form of DSE was created by deleting the first 31 amino- as well as the 58 carboxy-terminal amino acids. Consistently, the mean activity of the soluble mutant form of the enzyme was significantly decreased to mock control levels, in strong contrast to the wild-type enzyme (Supplementary Material, Fig. S5). Furthermore, the cell lysate from the patient-derived fibroblasts demonstrated a significant reduction in epimerase activity (Fig. 4). These results suggest that the DSE mutation p.S268L causes loss of epimerase activity, resulting in aberrant synthesis of DS chains and DS-PGs.

### The DSE mutation p.S268L causes a decrease in DS biosynthesis and leads to an increase in cellular CS chains

We compared the composition of CS/DS chains from patient and control fibroblasts in order to determine whether the DS biosynthesis was disturbed. In three sets of experiments, the GAG fractions from conditioned media and fibroblast lysates were digested with different chondroitinases to determine the amounts of DS moieties (Fig. 5 and Supplementary Material, Table S5), the amounts of CS moieties (Supplementary Material, Fig. S7 and Table S4) and CS and DS moieties together (Supplementary Material, Fig. S6 and Table S3). The CS/DS-derived disaccharides were fluorophore labeled and separated by anion-exchange HPLC, and the amount of disaccharides in each sample was calculated from the peak area in the chromatogram.

The results of all GAG measurements are summarized in Table 1. In accordance with an epimerase deficiency in mutant fibroblasts, we found a reduction in the IdoUA content of the CS/DS chains from the cell and culture medium fractions of the patient fibroblasts. The amount of DS disaccharides from the conditioned media was reduced to ~10% in the patient when compared with the control, whereas no apparent difference was observed in the amount of CS chains (Table 1). The amount of DS disaccharides obtained from the cell fraction was also reduced to ~20%, while CS-derived disaccharides was increased by ~1.5 times compared with the control cells (Table 1). This observation suggests that a reduction in the DS biosynthesis caused by the mutant DSE resulted in an increased synthesis of CS chains in the cell fraction or an accumulation of CS chains, which could not be converted to DS chains.

Our finding of a ~1.5 times larger amount of disaccharides liberated by chondroitinase ABC digest, corresponding to the total release of GlcUA and IdoUA linkages present, compared with the sum of separate releases of CS and DS disaccharides from the cell fraction indicated the presence of large amounts of otherwise rare linkage patterns, which were resistant to these enzymes. However, no significant difference was observed between the patient and the control with regard to the amount of larger oligosaccharides upon gel-filtration chromatography of the chondroitinase B digests of CS/DS chains of the cell and conditioned medium fractions from the fibroblasts (data not shown). Thus, the mutation of DSE results in the reduction in IdoUA clusters rather than sparsely distributed IdoUA residues in DS and CS/DS hybrid chains as was demonstrated in *Dse* null mice (46).

### The content of the IdoUA-GalNAc(4-*O*-sulfate)- structure characteristic for DS on decorin is reduced in the patient

We examined whether DSE deficiency affected the CS/DS hybrid chain on decorin, a major DS proteoglycan in the skin. The CS/DS hybrid chain on decorin is normally composed of a DS moiety (~95% as disaccharides) and a CS moiety (~5% as disaccharides) (27). A western blotting was performed for decorin core protein after digestion of the CS/DS hybrid chain with the

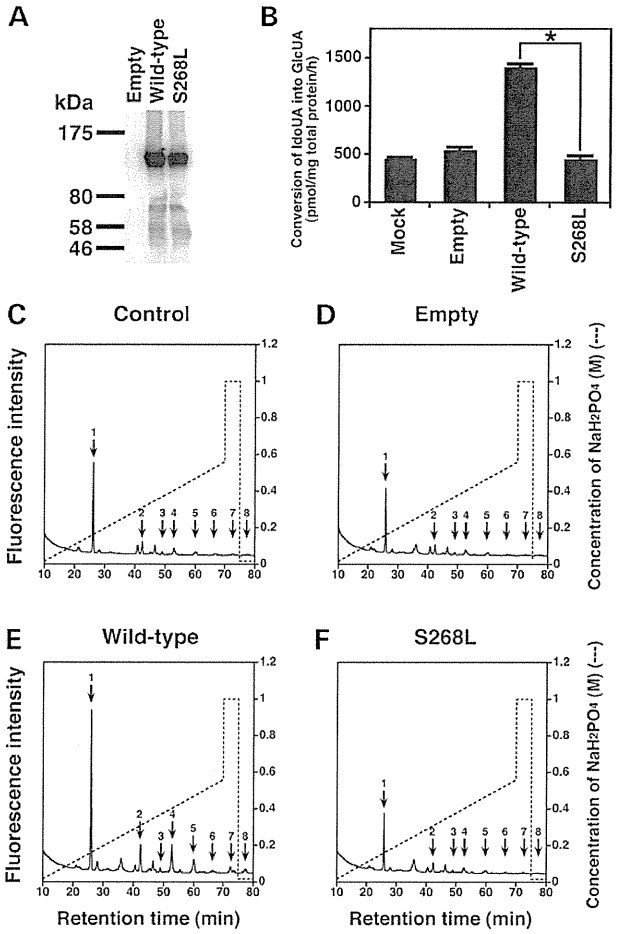


**Figure 3.** Expression and assays of the DSE activity of the full-length form of the recombinant DSE proteins (wild-type and p.S268L). (**A**) Western blotting of the recombinant DSE-V5 (wild-type and S268L). The recombinant DSE (wild-type and p.S268L) was transiently expressed in COS-7 cells, separated by 7.5% SDS–polyacrylamide gel electrophoresis, and detected with anti-V5 antibody. 'Empty' indicates the cell lysate from COS-7 cells transfected with an empty vector. (**B**) Comparison of the DSE activity of the full-length form of recombinant DSE (mean ± SE, $n = 3$). Enzyme assays were carried out as described in Materials and Methods. The strategy for the characterization of DSE reaction products is described in the legend to Supplementary Material, Figure S3. Briefly, the recombinant DSE (wild-type or mutant) was incubated with partially desulfated DS as the substrate. The DSE converts the IdoUA to GlcUA by its reverse-epimerizing activity, resulting in the formation of GlcUA residues, which are substituted by GalNAc residues. These linkages become susceptible to chondroitinase AC (Supplementary Material, Figs S3 and S4). After the incubation of the reaction products with chondroitinase AC, the resultant di- and oligo-saccharides such as ΔHexUA-GalNAc, ΔHexUA-GalNAc-IdoUA-GalNAc, ΔHexUA-GalNAc-IdoUA-GalNAc-IdoUA-GalNAc etc. were yielded. Each saccharide was labeled with a fluorophore (2-aminobenzamide) at the reducing terminus, and separated by anion-exchange HPLC (**C**–**F**). The ΔHexUA (4,5-unsaturated hexuronic acid) residue should be originally derived from a GlcUA residue due to the susceptibility to chondroitinase AC. Consequently, each saccharide contains a ΔHexUA at non-reducing end, and was utilized for quantifying the GlcUA content (Supplementary Material, Tables S6 and S7). The sum of each saccharide was described in the (B) with bar graphs. 'Mock' and 'empty' indicate the DSE activity from cell lysates of COS-7 cells transfected without and with an empty vector, respectively. $^*P <$ 0.0001 by Student's *t*-test. (C–F) Anion-exchange HPLC of the DSE reaction products prepared using the full-length form of recombinant DSE of wild-type (E) and p.S268L (F) and partially desulfated DS as substrate. Representative chromatograms from each reaction product are shown in the figure. (C )and (D) show the chromatograms of the substrate control and the reaction products of the cell lysate transfected with an empty vector, respectively. The DSE reaction products were digested with a mixture of chondroitinases AC-I and AC-II into di- and oligosaccharides, labeled with 2AB, and the 2AB-labeled oligosaccharides were separated by anion-exchange HPLC on an amine-bound silica PA-G column using a linear gradient of $NaH_2PO_4$ as indicated by the *dashed line*. The elution positions of authentic 2-AB-labeled di- and oligosaccharides derived from partially desulfated DS [Mikami *et al.* (21)] are indicated by numbered arrows: 1, ΔHexUA-GalNAc; 2, ΔHexUA-GalNAc-IdoUA-GalNAc; 3, ΔHexUA-GalNAc-IdoUA-GalNAc-IdoUA-GalNAc; 4, ΔHexUA-GalNAc-IdoUA-GalNAc(4S); 5, ΔHexUA-GalNAc-IdoUA-GalNAc-IdoUA-GalNAc(4S)/ΔHexUA-GalNAc-IdoUA-GalNAc(4S)-IdoUA-GalNAc; 6, ΔHexUA-GalNAc(4S)-IdoUA-GalNAc(4S); 7, ΔHexUA-GalNAc-IdoUA-GalNAc(4S)-IdoUA-GalNAc(4S); 8, 4-*O*-disulfated octasaccharide.

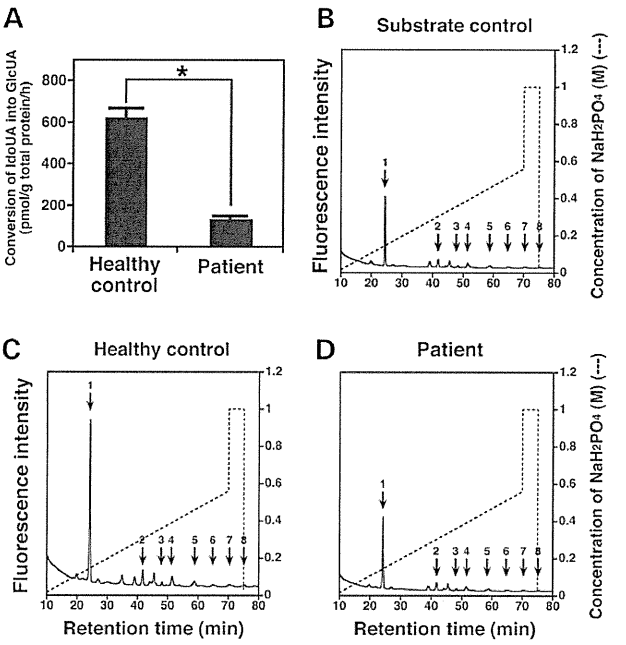


**Figure 4.** DSE activity in the skin fibroblasts from a healthy control and the patient. (**A**) Comparison of the DSE activity of the fibroblasts from a healthy control and the patient (mean ± SE, $n = 3$). The DSE reaction products were analyzed by anion-exchange HPLC (**B**–**D**). $^*P < 0.0005$ by Student's *t*-test. For the strategy of quantification of the DSE activity, see the legend to Figure 3. (B–D) Anion exchange HPLC of the DSE reaction products prepared using the cell lysate from the control (C) and the patient (D) and partially desulfated DS as substrate. Representative chromatograms from each reaction product are shown in the figure. (B) shows the chromatograms of the substrate control. The DSE reaction products were digested with a mixture of chondroitinases AC-I and AC-II into di- and oligosaccharides, labeled with 2AB, and the 2AB-labeled oligosaccharides were separated by anion-exchange HPLC as described in the legend to Figure 3. For the elution positions of authentic 2-AB-labeled di- and oligosaccharides, see the legend to Figure 3.

chondroitinases ABC, AC-I and B. The CS/DS hybrid chain on decorin was susceptible to all three types of chondroitinases, giving a single protein band in each case, which suggested that the side chain was of a CS/DS hybrid type. However, the molecular size of the band obtained using chondroitinase B appeared to be slightly larger, and that of the intact decorin proteoglycan much larger than that of the control (Fig. 6). This suggests that the GAG is larger than normal, and the cleavage site in the glycan

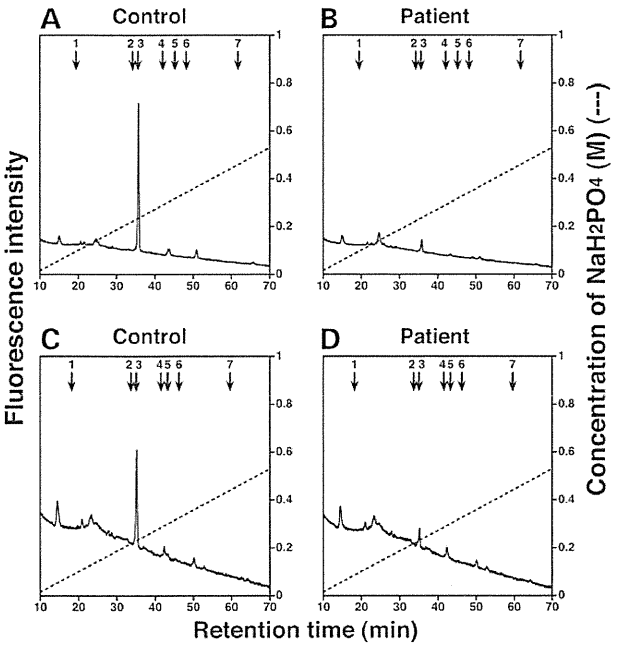


**Figure 5.** HPLC profiles of the digests of the GAG fractions prepared from the conditioned media (**A** and **B**) and cell fractions (**C** and **D**) of the fibroblast cultures after treatment with chondroitinase B. The GAG fractions containing CS/DS chains from a healthy control (A and C) and the affected individual (B and D) were digested with chondroitinase B, which specifically acts on the IdoUA-containing structure in DS or CS/DS hybrid chains, into disaccharides, labeled with 2AB, and 2AB-labeled CS/DS disaccharides were separated by anion-exchange HPLC on an amine-bound silica column using a linear gradient of $NaH_2PO_4$ as indicated by the *dashed line*. The elution positions of authentic 2-AB-labeled CS disaccharides are indicated by numbered arrows: 1, ΔHexUA-GalNAc; 2, ΔHexUA-GalNAc(6S); 3, ΔHexUA-GalNAc(4S); 4, ΔHexUA(2S)-GalNAc(6S); 5, ΔHexUA(2S)-GalNAc(4S); 6, ΔHexUA-GalNAc(4S,6S); 7, ΔHexUA(2S)-GalNAc(4S,6S).

chain for chondroitinase B is more distant to the glycan attachment site on the core protein than that of the cleavage sites for the other two enzymes. Although not unambiguously demonstrated by decorin western blotting, our findings of a reduced IdoUA content of cellular and secreted GAGs suggest that the content of the IdoUA-GalNAc(4-*O*-sulfate)- structure characteristic for DS on decorin is reduced in the patient.

### Rescue experiments performed by stable expression of wild-type *DSE* in patient fibroblasts increased the amount of secreted DS disaccharides

Stable expression vectors, pEBMulti-empty and -DSE (wild-type), were transfected into the patient cells, and the cells were propagated in the presence of G418. An analysis of DS chains was performed after digestion with chondroitinase B. The amount of DS disaccharides, ΔHexUA-GalNAc(4S), secreted by fibroblasts stably expressing DSE increased 3-fold compared with that obtained from cells transfected with the empty vector (Supplementary Material, Table S8 and Fig. S8). These observations strongly suggest that the patient shows a loss of function of *DSE*.

**Table 1.** The total amount of fibroblast-derived GAGs from CS/DS chains

| | CS/DS[a] | CS[b] | DS[c] | Hyaluronan[d] |
|---|---|---|---|---|
| Conditioned medium | nmol/mg protein | | | |
| Control | 47.9 | 29.9 | 18.3 | 68.5 |
| Patient | **16.2** | 20.8 | **1.7** | 85.3 |
| Cell fraction | nmol/mg protein | | | |
| Control | 1.2 | 0.90 | 0.33 | 7.2 |
| Patient | **2.2** | **1.4** | **0.066** | 4.1 |

Values, which showed clear or characteristic differences between the control and patient samples, are highlighted in bold.
[a]Total amount of disaccharides derived from CS/DS chains were calculated based on the peak area in the chromatograms of the digests with a mixture of chondroitinases ABC and AC-II (Supplementary Material, Fig. S6).
[b]Total amount of disaccharides derived from the CS moiety of CS/DS chains were calculated based on the peak area in the chromatograms of the digests with a mixture of chondroitinases AC-I and AC-II (Supplementary Material, Fig. S7).
[c]Total amount of disaccharides derived from the DS moiety of CS/DS chains were calculated based on the peak area in the chromatograms of the digests with chondroitinase B (Fig. 5).
[d]Total amount of disaccharides derived from hyaluronan were calculated based on the peak area in the chromatograms of the digests with a mixture of chondroitinases AC-I and AC-II (Supplementary Material, Fig. S7).

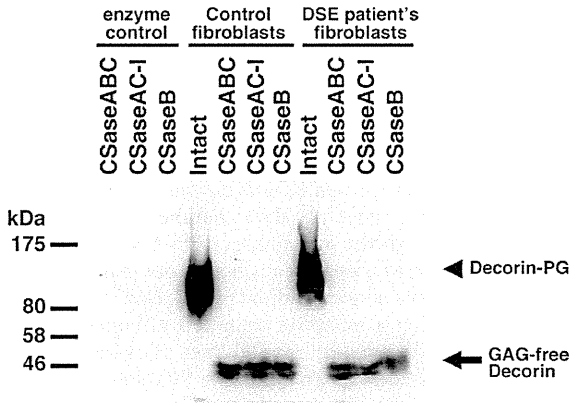


**Figure 6.** Composition of the CS/DS hybrid chain on decorin. A western blot was performed for decorin core protein after digestion of the CS/DS hybrid chain with the chondroitinases ABC, AC-I and B revealing that the side chain is of a CS/DS hybrid type. However, the molecular size of the band obtained using chondroitinase B may appears to be slightly larger, and that of the intact decorin proteoglycan is much larger than that of the control.

Taken together, our data indicate that the p.S268L mutation affects the epimerase activity, resulting in a decreased IdoUA content of DS chains, i.e. a reduced DS biosynthesis, and in an increased synthesis or an accumulation or reduced conversion of CS chains in the cell fraction, which cannot be converted to DS or hybrid CS/DS chains.

## DISCUSSION

*CHST14* mutations were recently identified in two distinct series of patients clinically diagnosed with a supposedly new form of EDS, named EDSKT (27), and with ATCS, and shown to result in D4ST1 deficiency (26). A comprehensive review of patients with D4ST1 deficiency reported to-date, variably diagnosed as ATCS, EDSKT and MCEDS, supports the notion that D4ST1 deficiency represents a single clinical entity, with some

degree of variability observed in inter- and intra-familial disease expression (28,36–38).

The disorder, MCEDS, is characterized by progressive multisystem fragility-related manifestations including joint dislocations and deformities, skin hyperextensibility, bruisability and fragility; recurrent large subcutaneous hematomas, and other cardiac valvular, respiratory, gastrointestinal, and ocular complications, which are considered to result from connective tissue weakness. The disorder also shows various developmental malformations including distinct craniofacial features, multiple congenital contractures and congenital defects in cardiovascular, gastrointestinal, renal, ocular and central nervous systems. MCEDS also affects muscles to a variable degree (38). MCEDS shares many clinical features with the kyphoscoliotic type of EDS (47), the tenascin-X deficient EDS (48), FKBP14-deficient EDS (41) and collagen VI-related Ullrich congenital muscular dystrophy (UCMD [MIM 254090]) and Bethlem myopathy (MIM 158810) (49). In addition, clinical overlap can be found at birth with distal arthrogryposis type 9 (congenital contractural arachnodactyly, CCA, Beals syndrome [MIM 121050]) due to FBN2 (MIM 612570) mutations and the Loeys-Dietz syndrome (LDS [MIM 609192]) within the first years of life. MCEDS can be diagnosed at birth by the presence of characteristic craniofacial features—consisting of brachycephaly, hypertelorism, down-slanting palpebral fissures, small mouth with thin vermillion border, prominent cheeks, microretrognathia and protruding ears—and distal arthrogryposis, and molecular genetic testing of *CHST14* was so far considered to provide a definitive diagnosis.

The patient we describe here presented with characteristic features of MCEDS, and we consequently show that there is locus heterogeneity in MCEDS: direct and indirect DNA analysis widely excluded *CHST14* as disease-causing in our patient, and the targeted analysis of a single candidate gene, *DSE*, from a linkage interval identified a missense mutation affecting a highly conserved residue. We present several lines of evidence that this mutation affects the DS eperimase's function. We show that the recombinant mutant enzyme's activity, as well as the patient-derived fibroblast's epimerase activity towards partly desulfated DS, is severely decreased. We observe decreased amounts of IdoUA-GalNAc(4-*O*-sulfate) linkages and increased amounts of GlcUA-GalNAc(4-*O*-sulfate) and GlcUA-GalNAc(6-*O*-sulfate) in the cellular and secreted GAG fractions of patient's fibroblasts after specific chondroitinase digests. We show that residual IdoUA-GalNAc(4-*O*-sulfate) linkages are present and unusually scattered over hybrid CS/DS chains. Fibroblasts with the p.S268L mutation in DSE epimerize GlcUA-GalNAc to IdoUA-GalNAc at a reduced rate resulting in secretion of about 10% IdoUA-containing disaccharides compared with a control. A significant fraction of DS is replaced by CS, which cannot generally substitute functions specifically associated with DS, as both D4ST1 and DSE deficiency causes MCEDS. Finally, we suggestively rescue the biochemical phenotype by stable expression of wild-type *DSE* in patient fibroblasts.

Conversion of GlcUA to IdoUA by DS epimerases is a freely reversible reaction that favors the GlcUA form, and the addition of sulfate to the C4 hydroxy of GalNAc adjacent to IdoUA by D4ST1 prevents further back epimerization of IdoUA to GlcUA (21,45). The notion of a spacio- and temporally coupled action of DSE and D4ST1 in the generation of IdoUA disaccharides and IdoUA blocks is supported by our reporting of MCEDS phenotypes resulting from deficiencies of either DSE or D4ST1, and both causing shortages of IdoUA residues in CS/DS chains in a number of connective tissues.

Apparently, DSEL cannot compensate for the loss of DSE function, analogous to the situation where CS 4-*O*-sulfotransferases cannot compensate for the loss of D4ST1, and in line with reported *in vitro* substrate specificities of human sulfotransferases involved in the 4-*O*-sulfation of CS/DS (20,21).

MCEDS might result both from abnormal and from loss of DS-proteoglycan functions. The structure of DS chains is more flexible than that of CS (50,51), which might affect DS proteoglycans such as decorin. Decorin directly binds to collagen via its core protein, and the GAG side chains aggregate and function as interfibrillar bridges (52,53). The observed connective tissue weakness in MCEDS patients might represent a direct consequence of insufficient decorin-mediated assembly of collagen fibrils caused by either D4ST1 or DSE deficiency. Indeed, we showed previously that the CS/DS side chain was replaced by a CS chain on the decorin molecule in skin fibroblasts from D4ST1-deficient patients and no DS moiety was detected (27). Similarly, our current study indicates that a deficiency of IdoUA residues in the decorin CS/DS chain results from DSE deficiency. Transition from the CS/DS hybrid chain of decorin to a CS chain probably decreases the flexibility of the GAG chain. Unfortunately, no material for electron microscopy of the skin is available from our patient. The rare studies of skin specimen from D4ST1-deficient patients showed that the size and shape of skin collagen fibrils were normal, but the collagen bundles appeared progressively and abnormally dispersed in the reticular dermis. The observation that dermal collagen fibrils showed huge varieties of size and shape in decorin null mice implicated the core protein of decorin as important for collagen fibril formation (54), and our findings suggest that the CS/DS hybrid chain of decorin regulates the space between the collagen fibrils and forms collagen bundles as indicated previously (27,55). This notion is supported by observing similar alterations, i.e. fibrils with larger diameter, in *Dse* null mice and in D4ST1-deficient skin when compared with controls (27,46). In line with our findings in the DSE-deficient patient, the amount of long IdoUA blocks was shown to be greatly decreased in decorin, biglycan and versican-derived CS/DS chains in *Dse* null mice (46). *Dse*-deficient mice were smaller than their wild-type littermates. All Dse null pups had a kinked tail that was not present after 4 weeks of age. Dse null mice showed otherwise no gross macroscopic alterations, but a reduced fertility (46). *Dsel* and *Dse* are expressed in all tissues in mice; *Dse* was the predominant epimerase in three of five tissues examined, i.e. the skin, lung and spleen, and the brain is the only tissue where most of the activity (89%) was attributed to Dsel (56,57). DSEL might encode the predominant epimerase in human brain as well, correlating with the absence of cognitive constraint in the patient. The amount of IdoUA in CS/DS proteoglycans varies between tissues and depends on the developmental stage (58,59); genetic and environmental factors, which contribute to its regulation, might explain some of the phenotypic variability observed between MCEDS patients.

Hypomorphic mutations in two enzymes involved in the synthesis of the GAG linker tetrasaccharide, encoded by *B4GALT7*

(MIM 604327) and *B3GAT3* (MIM 606374), result in deficiencies of more than one class of GAG chains, and cause the progeroid form of EDS (60–62) and a connective tissue disorder with multiple joint dislocations, short stature, craniofacial dysmorphism and congenital heart defects (63), respectively. MCEDS shares joint hypermobility with both conditions, and some facial features and an increased incidence of heart defects with the latter disorder, and this overlap might result from a reduction in the amount of DS proteoglycans.

The phenotypic overlap of MCEDS and the tenascin-X (TNX [MIM 600985])-deficient form of EDS (MIM 606408) (64) might be caused by a disruption of extracellular binding of decorin and tenascin-X, which also binds to tropoelastin and collagen types I, III, V, XII and XIV (65,66). In contrast to D4ST1 deficiency, where ecchymoses and hematoma formation are common (37), this was not observed in our young patient with DSE deficiency so far. A deficiency of DS is supposed to affect DS-mediated activation of heparin cofactor II (HCF2 [MIM 142360]) in the arterial wall after endothelial injury (67).

Quantitative and qualitative changes in the DS content of tissues are supposed to have effects on the generation of morphogen gradients in epithelia (5,6,68). For example, it has been shown that decorin neutralizes the activity of TGFB1 (69), and deficiency or substitution of DS chains by CS on decorin would implicate altered TGFB signaling in the pathogenesis of MCEDS, as it was shown in LDS (70) and Sphrintzen-Goldberg syndrome (SGS). Altered TGFB signaling might be responsible for features which are shared by LDS, SGS and MCEDS such as a Marfanoid habitus, hypertelorism, down-slanting palpebral fissures, arachnodactyly, joint hypermobility and joint contractures (71,72).

Of note, a DSE upregulation resulting in 5-fold increase in the CS/DS content and changes in growth factor binding and subsequently in pErk1/2 signaling have been found in esophagus squamous carcinoma, an aggressive tumor with poor prognosis, indicating that IdoUA in DS influences tumorigenesis by affecting cancer cell behavior (73). Upregulation of DSE has been observed in a number of other types of cancer as well (42).

We speculate that the variety of symptoms observed in MCEDS is caused by the deficiency of decorin and further DS proteoglycans, of which there are currently 29 known but less well studied than decorin, as well as due to the lack of DS in the vascular endothelia. The DSE and D4ST1 deficiencies represent disorders that specifically affect the DS biosynthesis, and emphasize roles of this GAG in human development and extracellular matrix maintenance (74).

## MATERIALS AND METHODS

### Patient and family

A 2-year-old Indian boy, born to healthy, consanguineous parents (first degree cousins), was clinically diagnosed with MCEDS based on the presence of facial dysmorphism, consisting of frontal bossing, open anterior fontanelle, downward-slanting palpebral fissures, telecanthus, bluish sclerae, high arched palate, tent-shaped lips, dental crowding, brachycephaly and prominent ears, as well as arachnodactyly, adducted thumbs, joint hyperlaxity, inguinal hernia and congenital bilateral talipes equino varus. Cardiac ultrasonography showed a patent foramen ovale, and a computed tomography of the brain showed a generalized mild cerebral atrophy. Following clubfoot surgery, the patient showed delayed wound healing and atrophic scarring of the skin. Generalized muscle weakness was observed pointing to an underlying myopathy. However, a muscle biopsy was not obtained. While his gross motor development was delayed, his cognitive development was normal.

### SNP array hybridization, homozygosity mapping and DNA sequence analyses

Written informed consent for molecular studies was obtained from the parents, and the study was conducted in accordance with the principles of the Declaration of Helsinki. Genomic DNA was isolated from peripheral blood leukocytes by standard procedures using a robot (BioRobot M48, QIAGEN). A genome-wide homozygosity scan and copy-number variant detection (molecular karyotyping) were performed following hybridization of the patient's DNA sample to a HumanCytoSNP-12v2 BeadChip SNP array (Illumina) interrogating 299 140 markers, and according to the manufacturer's instructions. Raw SNP call data were processed with the Genotyping Analysis Module of GenomeStudio 1.6.3 (Illumina). Copy-number variants and segments of loss of heterozygosity were called and visualized using Nexus software and the SNPFASST segmentation algorithm (BioDiscovery Inc.). A parametric multipoint logarithm of the odds score calculation was performed with the ALLEGRO program (75) using an autosomal recessive, fully penetrant model and marker allele frequencies determined out of 250 individuals of European descent from our in-house array facility.

The coding regions and splice sites of the CHST14 and DSE genes were PCR amplified and directly sequenced in our patient. Primer sequences were based on the NCBI reference entry for *CHST14* mRNA (NM_130468.3) and two available NCBI mRNA reference entries for *DSE* transcripts, which differ in their untranslated first exons (NM_001080976.1 and NM_013352.2). GoTaq polymerase and buffer (Promega, Mannheim, Germany) were used to PCR-amplify 20–50 ng of genomic DNA in 35 cycles of 20 s at 95°C, 20 s at 60°C and 30 s at 72°C in addition to an 7 min final extension, applied to all sets of primers (Supplementary Material, Table S1). The amplicons were cleaned using ExoSap-IT (USB, Vienna, Austria), and subsequently sequenced using an M13 universal primer on an ABI 3730s automated sequencer, with BigDye terminator mix (Applera, Vienna, Austria). Sequence chromatographs were analyzed using the Sequence Pilot computer program (JSI Medical Systems, Kippenheim, Germany). The parents and a healthy brother were tested for the mutation detected in the patient by sequence analysis. A panel of 300 Caucasian DNA samples from anonymous controls was analyzed for the presence of the identified *DSE* mutation by an allele-specific PCR (primers are shown in Supplementary Material, Table S2).

### Primary fibroblast cultures

We obtained skin fibroblasts from the patient at age 3 years, and an age-adjusted control. Cells were cultured in Dulbecco's modified Eagle's medium with 10% heat-inactivated fetal bovine serum, 100 U/ml penicillin, 100 U/ml streptomycin and 2 mM L-glutamine (Invitrogen).